Available online at www.sciencedirect.com
SCIENCE DIRECT®
Journal of Chromatography A, 1040 (2004) 97–104
JOURNAL OF CHROMATOGRAPHY A
www.elsevier.com/locate/chroma

Laser-induced breakdown detection combined with asymmetrical flow field-flow fractionation: application to iron oxi/hydroxide colloid characterization

Muriel Bouby*, Horst Geckeis, Thang Ngo Manh, Jong-Il Yun, Kathy Dardenne, Thorsten Schäfer, Clemens Walther, Jae-Il Kim

Forschungszentrum Karlsruhe, Institut für Nukleare Entsorgung, PO Box 3640, D-76021 Karlsruhe, Germany

Received 14 January 2004; received in revised form 24 March 2004; accepted 25 March 2004

Abstract

The combination of asymmetrical flow field-flow fractionation (AsFlFFF) with the laser-induced breakdown detection (LIBD) is presented as a powerful tool for the determination of colloid size distribution at trace particle concentrations. Detection limits (Dl) of 1, 4, and 20 μg/L have been determined for a mixture of polystyrene reference particles with 20, 50, and 100 nm in size, respectively. This corresponds to injected masses of 1, 4, and 20 pg, which is lower than found in a previous study with the symmetrical FlFFF (SyFlFFF). The improvement is mainly due to the lower colloid background discharged from the AsFlFFF channel. The combined method of AsFlFFF–LIBD is then applied to the analysis of iron oxi/hydroxide colloids being considered as potential carriers for the radionuclide migration from a nuclear waste repository. Our LIBD arrangement is less sensitive for iron colloid detection as compared to reference polystyrene particles which results in a detection limit of ∼240 μg/L FeOOH for the AsFlFFF–LIBD analysis. This is superior to the detection via UV-Vis absorbance and comparable to ICP-MS detection. Size information (mean size 11–18 nm) for different iron oxi/hydroxide colloids supplied by the present method is comparable to that obtained by sequential ultrafiltration and dynamic light scattering. A combined on-line ICP-MS detection is used to gain insight into the colloid-borne main and trace elements.

Keywords: Laser-induced breakdown detection; Flow field-flow fractionation; Field-flow fractionation; Colloids; Iron oxides

1. Introduction

The role of aquatic colloids is well known for the aquatic chemistry and migration of radionuclides and trace elements in aquifers [1–6]. Especially smaller sized particles with diameters <50 nm at trace concentrations, typical in natural water, are difficult to detect by conventional light scattering methods. Recent studies demonstrate that the laser-induced breakdown detection (LIBD) provides the highest sensitivity for the quantification of colloids with sizes down to 5 nm at concentrations below 1 ppt [7,8]. The principle of the method is based on the interaction of a focused pulsed laser beam with solid particles dispersed in the sample solution. At an appropriate power density (around 10^{10} W/cm^2), a dielectric breakdown generating a plasma occurs selectively within the solid particle. The emitted light and shock wave accompanying the plasma formation can be detected for the determination of colloid concentration and average size [9–12]. However, the characterization of colloid dispersion of multimodal size distribution with unknown composition turns out to be difficult to resolve from the LIBD signal alone. Particularly for the analysis of natural aquatic samples, a size fractionation prior to LIBD detection appears to be necessary to obtain quantitative results on colloid size and concentration. Characterization of natural aquatic colloids by the flow field-flow fractionation is described by a number of authors [13–19]. Size fractionation is achieved in a thin ribbon like channel in a laminar carrier flow, applying a cross-flow perpendicular to the channel flow. The elution sequence of colloidal species is determined by their diffusion coefficient and consequently by their size. A major advantage of the method is the absence of a stationary

* Corresponding author. Tel.: +49-7247-82-4939; fax: +49-7247-82-3927.
E-mail address: bouby@ine.fzk.de (M. Bouby).

0021-9673/$ – see front matter © 2004 Elsevier B.V. All rights reserved.
doi:10.1016/j.chroma.2004.03.047

phase, thus, limiting the effects of an interaction between the sample components and the equipment surfaces [20–22].

The colloid determination after size fractionation can be accomplished by various detection systems. For the low colloid concentrations in natural water samples, the currently used light scattering, or refractive index detectors, appear to be unsuitable. If the concentration is not so low, colored species as ferrihydrite and humic colloids can be sensitively detected by UV-Vis spectrophotometry. The combination of a flow field-flow fractionation method with ICP-mass spectrometry (ICP-MS) provides the information on the inorganic element content of different colloid size fractions. This combination has already been reported to impart valuable insight into the metal ion colloid interaction [19,23]. The addition of LIBD as a detection system to the symmetrical flow field-flow fractionation (SyFlFFF) has been successfully applied to the analysis of a polystyrene reference colloid mixture [24] and also with the asymmetrical flow field-flow fractionation (AsFlFFF) to the characterization of humic colloid containing natural groundwater [19]. The previous SyFlFFF study, however, suffered from problems of colloid release from channel components that increases the background signal [24].

In the first part of the present work, the detection limit of the AsFlFFF–LIBD combination is specified by analyzing mixtures of well characterized polystyrene reference colloids. This experiment is performed to test the method and to allow the direct comparison of the outcome with the results of the earlier SyFlFFF studies. The method is then applied to the size determination of iron oxi/hydroxides colloids as they are generated from secondary phases of the weathered igneous and sedimentary rocks [25] and also from precipitates in Fe-bearing waters [26]. Such aquatic colloids are influencing the migration behavior of heavy metal cations and radionuclides in natural aquifer systems, and thus, are considered as possible carriers for the radionuclide propagation from a nuclear waste repository [6,27–31]. Colloid size is one of the important parameters which have to be known in order to assess their mobilizing influence on radionuclides.

2. Experimental section

2.1. Samples

Stock solutions of reference polystyrene particles of three different sizes 20 nm (21 ± 1.5), 50 nm (50 ± 2), and 100 nm (102 ± 3) (Duke Scientific Corporation, California, USA) were prepared in ultrapure water (Millipore, MilliQ Plus). Different mixtures for calibration were then obtained by appropriate dilution of these stock solutions (see Table 1).

Two 6-Line ferrihydrite (6LFh) solutions synthesized according to the known procedure [32] are investigated for their colloidal suspension. These solutions are named old 6LFH and new 6LFh related to their aging time for 30 and 9 months, respectively. XRD pattern (Seifert 3000TT) are found to be identical for both samples, showing broadened lines at 0.15, 0.17, 2.00, 2.25, and 2.54 nm, being characteristic of the 6LFh [32]. This reveals that no alteration of the 6LFh stock solutions occurred during this period. Another colloidal dispersion originating from the transformation of 2-Line ferrihydrite (2LFh) in presence of Lu^{3+} to hematite (68%) and goethite (32%) [33] has been also investigated.

Table 1
Polystyrene particles concentrations in the different mixtures

Mixture	20 nm (μg/L)	50 nm (μg/L)	100 nm (μg/L)
A	10	100	1000
B	5	50	500
C	2	20	200
D	1	10	100
E	MilliQ water		

2.2. Instrumentation

2.2.1. Asymmetrical flow field-flow fractionation (AsFlFFF) combined with UV-Vis, ICP–MS, and LIBD detection

The general principles of the field-flow fractionation methods are described in details elsewhere [21–22]. A more detailed description of the AsFlFFF can be found in [14,15,22,34–37]. In this study, the AsFlFFF system is provided by Postnova Analytics (HRFFF 10.000 AF4). The accumulation wall of the channel is made of an ultrafiltration membrane from regenerated cellulose with a 5 kDa pore size (Postnova Analytics). The PTFE spacer of 0.5 mm in height delimits the channel thickness. A solution of 1 mmol/L MES buffer (2-(*N*-morpholino)ethanesulfonic acid) at pH (4.6 ± 0.1) is used as a carrier, which is degassed prior to use by a vacuum degasser. The channel flow rate is maintained at 0.35 or 1 ml/min, during the fractionation of the polystyrene mixture or the iron colloids, while the cross-flow is kept constant at 0.25 ml/min for 30 min or at 0.67 ml/min for 10 min, respectively.

The sample solutions are ultrasound treated and passed through a 450 nm syringe filter before injection (injected sample volume: 100 μl). The injected sample is then focused during 2 min before the elution starts. From the channel, the effluent is directed through an UV-Vis detector (Postnova Analytics), recording the absorption signal simultaneously at three different wavelengths: 210, 254, and 400 nm. For the determination of detection limits we took the wavelength which showed highest absorbance values. At the low particle concentrations investigated in our experiments, ferrihydrite colloids could only be detected at $\lambda = 210$ nm. Under given conditions, light attenuation for ferrihydrite and polystyrene colloids is due to both effects, light scattering and absorption. From the UV-Vis detector the sample is led to the flow-through cell (750 μl) of the LIBD. A detailed description of the LIBD apparatus is available from refs. [10,19,24].

A pulsed laser beam (Continuum surelite I) with a repetition rate of 20 Hz at the second harmonic wavelength (532 nm) is focused into a silica cuvette containing the sample solution via a plano-convex lens of 50 mm focal length. As already discussed in [24], the detection volume is restricted to the effective focus volume of the laser beam which is in the pL range [8]. This together with the fact that there is obviously only insignificant mixing in the detector cuvette the resolution is comparable to that of the other detectors. The laser pulse energy is adjusted to 0.35 mJ by a variable attenuator. This laser pulse energy represents a threshold value where no breakdown is induced in ultrapure water. The plasma generated at a breakdown event is monitored by a macro-microscope equipped with a CCD monochrome camera triggered by the incident laser pulse and recorded by a PC controlled picture processing system. The breakdown probability is defined as the ratio of the plasma generation events to the number of laser pulses. During the fractionation the breakdown probability is evaluated by averaging breakdown events observed for 1000 laser pulses. The resulting fractograms are plotted as a function of the elution time. For the analysis of the colloid element composition, the ICP-MS and replaces the LIBD. The effluent is then mixed via a T-piece with 6% nitric acid containing 100 μg/L Rh as an internal standard and introduced into the ICP-MS (Perkin-Elmer, ELAN 6000) at a constant rate of 0.5 ml/min. Colloid size information is derived from the calibration with a mixture of polystyrene colloids.

2.2.2. Symmetrical flow field-flow fractionation (SyFlFFF) combined with laser light scattering (LLS)

For comparison one sample of the new 6LFh is analyzed by the application of a SyFlFFF–LLS arrangement. This equipment is described in detail elsewhere [16,24] and see [20,22] for more detailed informations about the SyFlFFF method. The carrier solution is the same as used in AsFlFFF. Channel- and cross-flow rates are maintained at 1 ml/min throughout this work. The injected sample volume is 20 μl. A stop-flow procedure is used for sample relaxation. The sample is injected into the top of the SyFlFFF channel and only the cross-flow with no channel flow is applied for 2 min. The fractionator used is a model F-1000 from FFFractionation Inc. (Salt Lake City, USA). The lower frit of the channel (27.4 cm “effective” length, 2.0 cm width) is covered with a membrane consisting of regenerated cellulose with C.O. 5 kDa from Schleicher & Schuell (Dassel, Germany). The carrier is degassed by a 1100 Series Vacuum Degasser model G 1322A and delivered at constant rates to the fractionator by a 1100 HPLC Iso-pump model G 1310A from Hewlett-Packard (Waldbronn, Germany). From the channel, the effluent is directed through a LLS-detector. The cross-flow is provided by a double piston precision pump P-500 from Pharmacia Biotech AB (Sweden) in a re-circulating cross-flow loop.

In this study, laser light scattering detection is performed by a commercial DAWN-DSP-F light scattering photometer from Wyatt Technology Corp. (Santa Barbara, USA). A 5 mW HeNe laser provides the incident light beam (λ_{em} = 632 nm) and is directed through the detector cell of 70 μl volume. Scattered light is detected by an array of 18 photodiodes arranged at different angles relative to the incoming laser beam. Only the signal detected by the 90° detector is taken for the present study. The size of the colloids is calculated by applying the approximated relation given in [22] relying the diffusion coefficient to the retention volume ($V_r = v_c w^2/6D$; V_r: retention volume; v_c: volumetric cross-flow; w: channel width, and D: diffusion coefficient).

Additional size determinations have been conducted by photon correlation spectroscopy (PCS) using a homodyne (single-beam) ZetaPlus system (Brookhaven Inc.) equipped with a 50 mW solid-state laser (λ_{em} = 632 nm) and by sequential filtration through filters of 200, 450 nm pore size (Cellulose Acetate syringe filters from Novodirect) and ultrafilters with the following cut-offs 1000, 300, 100, 50, and 10 kDa, respectively (filter cartridges from Pall Filtron). Assuming spherical shape of the analyzed colloids, these cut-off values can be attributed to the respective hydrodynamic diameters of 17, 11, 7.4, 5.3, and 3 nm [38].

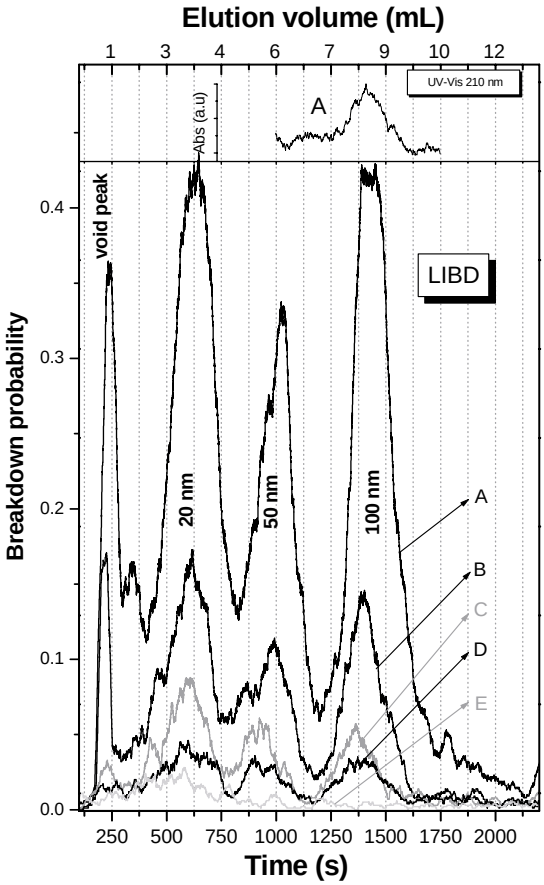

Fig. 1. AsFlFFF fractionation of polystyrene particle mixtures detected by LIBD and UV-Vis (inserted in the upper part). Details for abbreviations A, B, C, D, and E can be found in Table 1.

3. Results and discussion

3.1. Fractionation of polystyrene particles

Standard particles of three sizes (20 nm/50 nm/100 nm) are mixed for concentrations varying from (10/100/1000) down to (1/10/100) μg/L, respectively. The particle concentrations are given in Table 1. The fractograms for standard polystyrene particle mixtures obtained by AsFlFFF are shown in Fig. 1. The separation of different particle sizes is clearly distinguished and the breakdown probability follows a linear relationship with the colloid concentration. Breakdown probability data for the peak maxima in the fractogram (Fig. 1) are plotted versus the particle concentration in Fig. 2. From the scatter of the blank fractogram (E in Fig. 1) obtained by injecting ultrapure water, detection limits can be estimated by calculating the threefold standard deviation of the background data in the peak range. Detection limits of 1 μg/L for the 20 nm, 4 μg/L for the 50 nm and 20 μg/L for the 100 nm particles are obtained. This corresponds to 1, 4, and 20 pg, respectively, in terms of injected masses. The detection limits for the 50 and 100 nm particles are, thus, improved compared to previous results obtained with the SyFlFFF–LIBD arrangement which were in concentration terms 2, 40, and 240 g/L for the 20, 50, and 100 nm particles, respectively, or 1, 8, 48 pg in terms of injected masses. The improvement is mainly due to the better resolution and to the lower background generated by the AsFlFFF method. Previous studies with the SyFlFFF–LIBD arrangement suffered from a rather high background induced by corrosion of the ceramic frits overlying the fractionation channel. The AsFlFFF does not contain this frit, and hence, the background breakdown probability is decreased from ∼30 to <5%. Nevertheless, the detection limit for the 20 nm particles is still affected by the increased background in the peak elution region due to either detritus from the membrane or residues from earlier injections. A further decrease of the detection limit will, therefore, be very dependent on the successful suppression of such interferences.

Even though we used a carrier of low ionic strength, it is important to note that there is no sample concentration effects observed in the peak positions. Such shifts of the peak position to earlier elution times are a common observation in case of overloading the channel or for charged particles due to charge repulsion effects [16,22,39]. In our present study, the mass overloading effects can be excluded under the low concentration conditions investigated here and the surface charge of the reference colloids is obviously not influencing the peak positions. The reproducibility of peak positions even at lowest concentrations indicates furthermore that no significant retardation of the particles occurs at the membrane surface shifting the peak maxima to later elution times. UV-Vis spectrophotometric detection ($\lambda = 210$ nm) could only identify the position of the 100 nm particles in the highest concentrated mixture at the same location as the LIBD peak. This finding verifies that colloid interaction with tubing connections between UV-Vis and LIBD detector does not play a significant role.

3.2. Fractionation of iron colloids

Figs. 3–5 present the fractograms detected by UV-Vis, LIBD, and ICP-MS for the iron oxi/hydroxide solutions. The stock solutions have been diluted by the carrier solution before injection to the final concentrations of 2.45, 5.22, and 4.65 mg/L for the old 6LFh, the new 6LFh and the transformed 2LFh, respectively. This represents in terms of injected masses 245, 522, and 465 ng, respectively, for a total injection volume of 100 μl. The UV-Vis fractograms are obtained by the absorbance measurement at 210 nm as

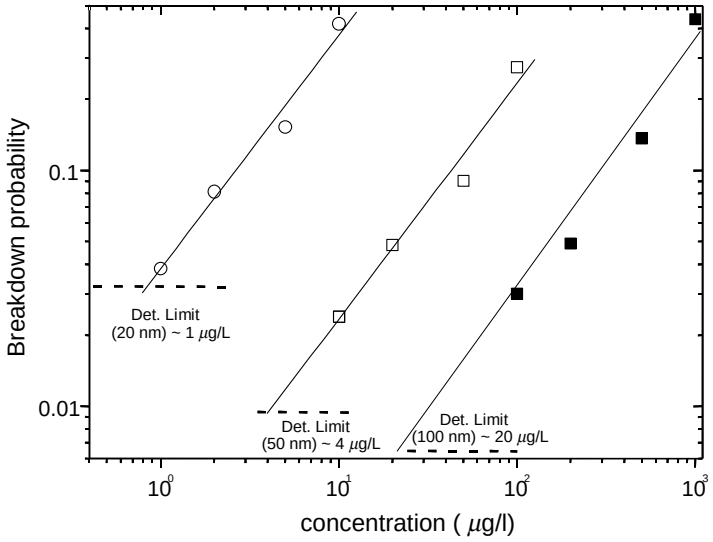

Fig. 2. Relation of the breakdown probability (peak height in the fractogram, Fig. 1) to the particle concentration. Detection limits are estimated from the threefold standard deviation of the blank fractogram.

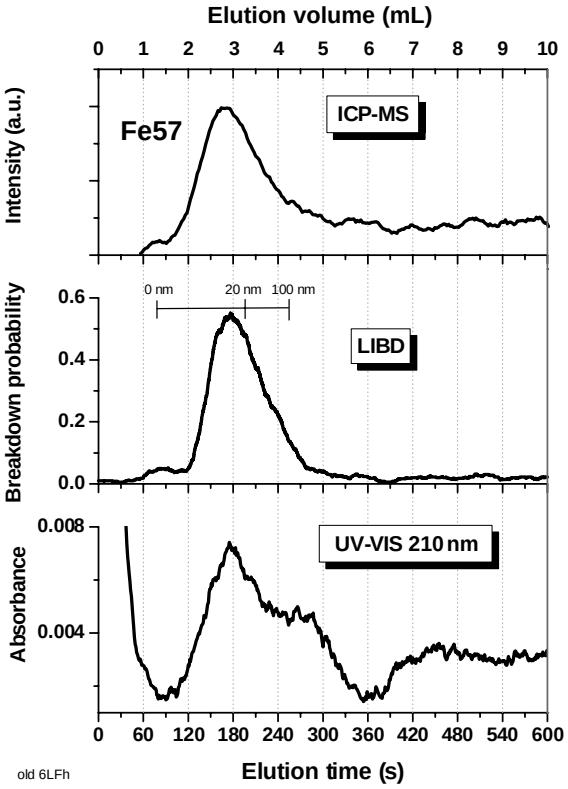

Fig. 3. AsFlFFF–UV-Vis/LIBD/ICP-MS fractograms of the old 6LFh.

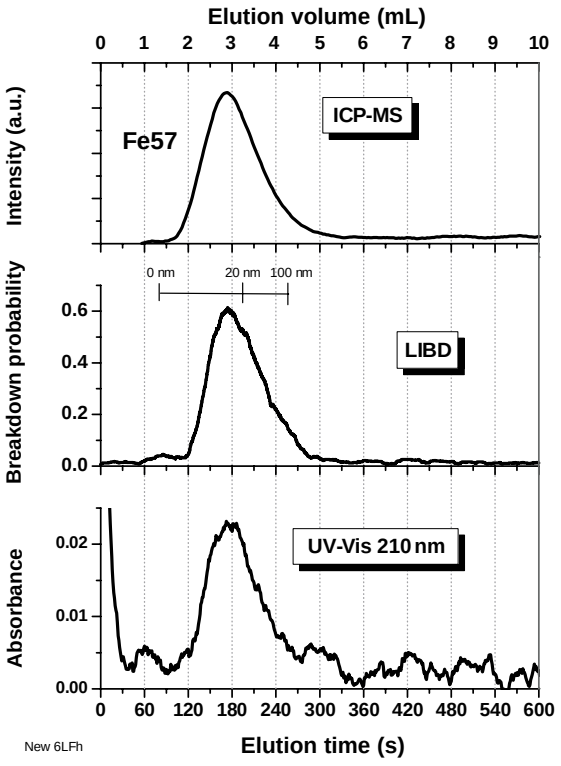

Fig. 4. AsFlFFF–UV-Vis/LIBD/ICP-MS fractograms of the new 6LFh.

indicated in all figures. ICP-MS detection is made by measuring Fe-57, as the iron determination at 57 amu is less prone to interferences by molecule ion formation as found for Fe-56. Lu-175 is additionally monitored in case of the 2LFh transformed to hematite/goethite in the presence of Lu(III). The LIBD fractograms are obtained as explained in Section 2 and contain size information related to the calibration with reference polystyrene particles. Fig. 6 shows for comparison the SyFlFFF–LLS fractograms for the new 6LFh.

At the low colloid concentrations applied in the experiment, UV-Vis detection appears to be close to the detection limit. Detection limits calculated in the same way as described above for the polystyrene particles lie at ∼240 μg/L for the LIBD, at ∼380 μg/L for the ICP-MS and at ∼800 μg/L for the UV-Vis absorbance. For the calculation, it is assumed that the colloid composition corresponds to FeOOH. Even though it is still possible to detect the FeOOH colloids by AsFlFFF–LIBD in the upper μg/L range, the detection sensitivity of the available LIBD arrangement for those iron colloids is much lower than for polystyrene particles. This fact suggests that higher laser energy is required to initiate the dielectric breakdown in the FeOOH colloids due to insufficient particle density or due to properties of the solid which inhibit the generation of a plasma under given laser parameters. More studies are necessary to elucidate this phenomenon quantitatively.

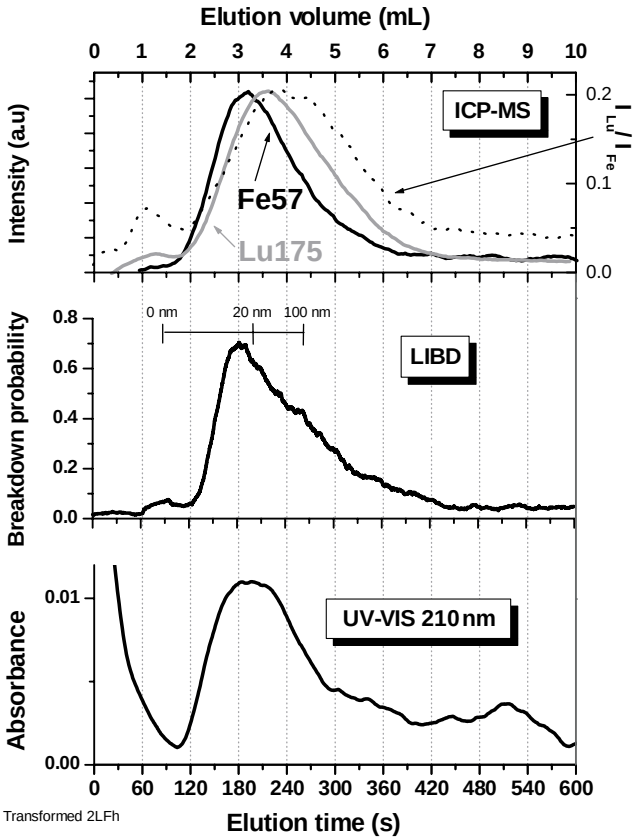

Fig. 5. AsFlFFF–UV-Vis/LIBD/ICP-MS fractograms of the transformed 2LFh; the dotted line in the ICP-MS fractogram represents the intensity ratio for the Lu/Fe ICP-MS signal.

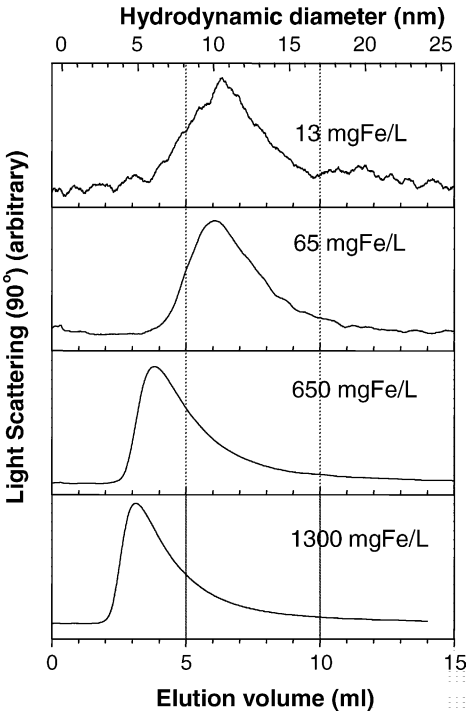

Fig. 6. SyFlFFF–LLS fractograms of the new 6LFh obtained at different colloid concentrations.

For the two differently aged 6LFh solutions, as shown in Figs. 3 and 4, the fractograms exhibit a more or less symmetric peak with a maximum at 170 s (2.8 mL) indicating a quite monomodal size distribution of the predominant colloid population. In general, the detector response for light scattering, LIBD and ICP-MS are known to be very different for varying colloid sizes (see e.g. [17,19]). The rather similar fractograms obtained by the different detector types, therefore, strongly support the conclusion that the 6LFh colloids have a rather narrow colloid size distribution. No peak shift due to overloading effects is observed when injecting colloids in the low concentration range from 1 up to 15 mg/L (not presented here). During the SyFlFFF–LLS studies, such an effect is clearly visible at colloid concentrations >13 mg/L (Fig. 6). Lower colloid concentrations are difficult to detect by the detection systems (UV-Vis absorption and LLS) available for SyFlFFF. Correction for the concentration effect by extrapolation to low colloid concentrations results in a mean size for the colloids at peak maximum at 11 nm for the SyFlFFF–LLS study. Fourteen to fifteen nanometers are obtained from the AsFlFFF–LIBD/ICP-MS experiment. The differences may partly derive from the different ways of calibration. AsFlFFF has been calibrated by polystyrene reference colloids. Results of the SyFlFFF–LLS analysis are obtained from the given theoretical relationship between elution volumes and diffusion coefficient [22] (see Section 2). Characterization of 6LFh colloids by TEM and electron nanodiffraction reported in the literature so far [40,41] resulted in typical sizes for the primary crystallites of $\leq$6 nm. It is, therefore, reasonable to assume that the particles studied here are small agglomerates rather than primary crystallites. It has to be noted that the derived sizes are sphere related. It is known that low crystalline iron oxy-hydroxide colloids show a broad variety of shapes so that the sizes here have to be considered as estimates.

The fractograms of the 2LFh solution in Fig. 5 are slightly different from those obtained for the two 6LFh solutions and also show differences with regard to the detection method. In this case, the peaks are more asymmetric with a maximum at 190 s (3.2 mL) followed by a tailing up to 420 s (7 mL). This, together with the variation in fractogram shape obtained by the different detector types, is a clear indication for the presence of larger sized colloids in the sample. According to the size calibration relative to polystyrene particles, the major part of the iron colloids after 450 nm filtration has a diameter of around 18 nm, whereas minor fractions range up to around 100 nm in size. The 2LFh transformation leads to the formation of 68% of hematite and 32% of goethite [33]. Goethite is known to form elongated needle like crystals of a length of several hundred nanometers. This was confirmed by AFM images shown in [33]. They are, thus, not observed in AsFlFFF due to the prefiltration at 450 nm. Scanning electron microscopy suggests that the hematite itself is composed of smaller spherical particles in a size range up to 40–60 nm [33]. These are those mainly observed in this study. In this case the independent information on the colloid shape substantiates the assumption of spherical particles. The ICP-MS signal for Lu reacted with 2LFh follows the Fe-signal, thus, demonstrating the attachment of Lu(III) to colloids. However, a clear shift is observed in the Lu fractogram relative to the Fe-fractogram with a maximum at 220 s (3.6 mL) corresponding to a size of 50 nm. Such finding has already been stated in case of humic colloid borne lanthanides and actinides [19] and is taken as an indication that the metal ion may be included into the colloid structure, however, not homogeneously distributed within the different colloid size fractions with a fixed Lu/Fe ratio. The dotted line in the ICP-MS fractogram in Fig. 5 represents the Lu/Fe ratio which shows a maximum at 240 s (4 mL) at a size of 68 nm. This finding indicates a preferential incorporation of Lu(III) into the hematite colloids in this size range as suggested by the X-ray absorption (EXAFS) study [33].

Ultrafiltration experiment corroborates the size information obtained by AsFlFFF as shown in Fig. 7. Less than ~20% of iron is found in the filtrate at pore sizes below 11 nm in all samples and a fraction of 70–100% of the two different 6LFh colloid types passes the 1000 kDa cut-off filter (corresponding to a pore size of about 17 nm according to [38]). Taking into account that the conversion of the filter cut-off to a hydrodynamic size is afflicted by some uncertainties, filtration supports the size information provided by AsFlFFF. Filtration of the transformed 2LFh exhibits less than 15% of colloids being smaller than 17 nm. This again reflects the presence of particles larger than those found in the 6LFh solution. Twenty percent of colloids in 2LFh are

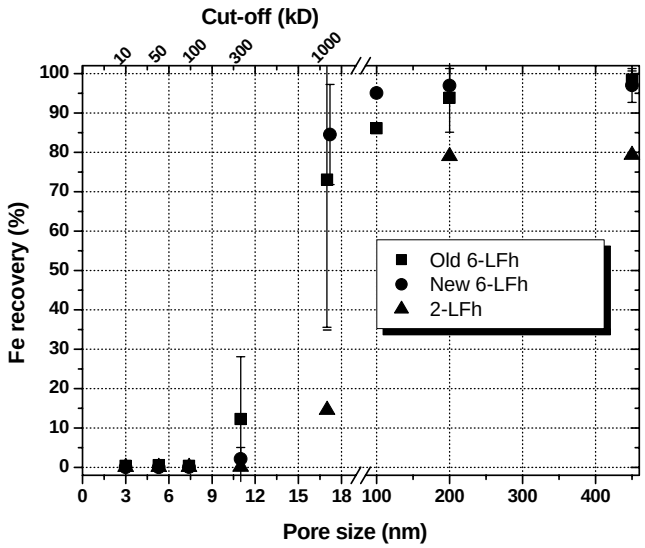

Fig. 7. Results of filtration of the iron colloids.

already separated by filtration at 450 nm pore size. This can be related once more to the 2LFh composition. The XRD study indicates the formation of 68% of hematite and 32% of goethite upon the 2LFh transformation [33]. The latter species are known to form elongated needle like crystals of larger size as already mentioned earlier. These are assumed to be separated by the 450 nm filtration. The predominant size group deduced from the fractogram, with a major fraction found between 18 and 100 nm, agrees with ultrafiltration results. The larger particles are separated by 450 nm filtration prior to the injection into the channel. A minor concentration of particles between 200 and 450 nm appearing as a tailing in the fractogram (Fig. 5) undergoes partial sorption onto the membrane during the focusing and fractionation steps. This is verified by the inspection of the membrane after a series of fractionations, revealing a brown reddish coloring of the membrane around the injection region.

The colloid sizes obtained by PCS after 450 nm filtration also confirm the results discussed above. The PCS size ranges from 5 to 20 nm for the old 6LFh and very similar for the new 6LFh (5–25 nm). In agreement with other experiments, 2LFh is found to cover a larger size range up to 100 nm.

4. Conclusions

The detection limits of the AsFlFFF–LIBD combination are determined after fractionation of polystyrene colloid mixtures in the trace concentration range. Lower detection limits are achieved as compared to earlier experiments with a SyFlFFF–LIBD arrangement due to the lower colloid background released from its channel components. For the iron oxihydroxide colloids, a much lower sensitivity of LIBD detection is found. The reasons for that observation has to be studied further.

The AsFlFFF–LIBD combination appears to be a helpful tool for the characterization of colloid dispersions with particle concentrations in the upper μg/L range. A further improvement of the detection limit is still possible by injecting a larger sample volume and by performing a preconcentration. Even for colloids of intense color as in the case of ferrihydrites, LIBD appears to be a colloid detector superior to spectrophotometry. The use of ICP-MS detection appears to be a valuable method for the investigation of metal ion interaction with aquatic colloids.

References

[1] J.I. Kim, Radiochim. Acta 52/53 (1991) 71.
[2] J.I. Kim, MRS Bull. XIX 12 (1994) 47.
[3] B.D. Honeyman, Nature 397 (1999) 23.
[4] R. Artinger, W. Schuessler, T. Schäfer, J.I. Kim, Environ. Sci. Technol. 36 (20) (2002) 4358.
[5] W. Hauser, H. Geckeis, J.I. Kim, Th. Fierz, Colloids Surf. A 203 (2002) 37.
[6] T. Schäfer, R. Artinger, K. Dardenne, A. Bauer, W. Schuessler, J.I. Kim, Environ. Sci. Technol. 37 (8) (2003) 1528.
[7] T. Kitamori, K. Yokose, K. Suzuki, T. Sawada, Y. Gohshi, Jpn. J. Appl. Phys. 27 (3) (1988) L983.
[8] F.J. Scherbaum, R. Knopp, J.I. Kim, Appl. Phys. B 63 (1996) 299.
[9] W. Hauser, T. Bundschuh, Patent: DE 198 33 339 (2000).
[10] T. Bundschuh, W. Hauser, J.I. Kim, R. Knopp, F.J. Scherbaum, Colloids Surf. A 180 (2001) 285.
[11] T. Bundschuh, R. Knopp, J.I. Kim, Colloids Surf. A 177 (2001) 47.
[12] C. Walther, C. Bitea, W. Hauser, J.I. Kim, F.J. Scherbaum, Nucl. Instrum. Methods B 195 (3–4) (2002) 374.
[13] R. Beckett, Z. Jue, J.C. Giddings, Environ. Sci. Technol. 21 (3) (1987) 289.
[14] C. Tank, M. Antonietti, Macromol. Chem. Phys. 197 (1996) 2943.
[15] M.E. Schimpf, M.P. Petteys, Colloids Surf. A 120 (1997) 87.
[16] T. Ngo Manh, H. Geckeis, J.I. Kim, H.P. Beck, Colloids Surf. A 181 (1–3) (2001) 289.
[17] M. Plaschke, T. Schäfer, T. Bundschuh, T. Ngo Manh, R. Knopp, H. Geckeis, J.I. Kim, Anal. Chem. 73 (17) (2001) 4338.
[18] A. Siripinyanond, R.M. Barnes, D. Amarasiriwardena, J. Anal. At. Spectrom. 17 (2002) 1055.
[19] M. Bouby, T. Ngo Manh, H. Geckeis, F.J. Scherbaum, J.I. Kim, Radiochim. Acta 90 (2002) 727.
[20] J.C. Giddings, F.J. Yang, M.N. Myers, Anal. Chem. 48 (8) (1976) 1126.
[21] J.C. Giddings, Science 260 (1993) 1456.
[22] M.E. Schimpf, K. Caldwell, J.C. Giddings (Eds.), Field-Flow Fractionation Handbook, Wiley-Interscience, Wiley, New York, 2000.
[23] M. Hasselöv, B. Lyven, C. Haraldsson, W. Sirinawin, Anal. Chem. 71 (1999) 3497.
[24] T. Ngo Manh, R. Knopp, H. Geckeis, J.I. Kim, H.P. Beck, Anal. Chem. 72 (2000) 1.
[25] J.L. Jambor, J.E. Dutrizac, Chem. Rev. 98 (1998) 2549.
[26] R.M. Cornell, U. Schwertmann, The Iron Oxides—Structure, Properties, Reactions, Occurrence and Uses, VCH-Verlag, Weinheim, 1996.
[27] L.W. Lion, R.S. Altmann, J.O. Leckie, Environ. Sci. Technol. 16 (1982) 660.
[28] R.J. Davies-Colley, P.O. Nelson, K.J. Williamson, Environ. Sci. Technol. 18 (1984) 491.
[29] N. Lu, K.S. Kung, C.F.V. Mason, I.R. Triay, C.R. Cotter, A.J. Pappas, M.E.G. Pappas, Environ. Sci. Technol. 32 (1998) 370.
[30] T.E. Payne, J.A. Davis, T.D. Waite, Radiochim. Acta 66/67 (1994) 297.

[31] C.E. Barnes, J.K. Cochran, Geochim. Cosmochim. Acta 57 (1993) 555.
[32] U. Schwertmann, R.M. Cornell, Iron Oxides in the Laboratory (Preparation and Characterization), VCH-Verlag, Weinheim, 1991.
[33] K. Dardenne, T. Schäfer, P. Lindqvist-Reis, M.A. Denecke, M. Plaschke, J. Rothe, J.I. Kim, Environ. Sci. Technol. 36 (23) (2002) 5092.
[34] K.-G. Wahlund, J.C. Giddings, Anal. Chem. 59 (1987) 1332.
[35] A. Litzen, K.-G. Wahlund, Anal. Chem. 63 (1991) 1001.
[36] T. Schauer, Part. Part. Syst. Charact. 12 (1995) 284.
[37] P.S. Williams, J. Microcol. Sep. 9 (1997) 459.
[38] P. Andrews, Biochem. J. 91 (1964) 222;
P. Andrews, Biochem. J. 96 (1965) 595;
P. Andrews, Methods Biochem. Anal. 18 (1970) 1.
[39] J.E. Wijnhoven, J.P. Koorn, H. Poppe, W.Th. Kok, J. Chromatogr. A 699 (1995) 119.
[40] R.A. Eggleton, R. Fitzpatrick, Clay Clay Miner. 36 (2) (1988) 111.
[41] D.E. Janney, J.M. Cowley, P.R. Buseck, Clay Clay Miner. 48 (1) (2000) 111.